

Thermal vibrational convection in near-critical fluids. Part 1. Non-uniform heating

By D. LYUBIMOV¹, T. LYUBIMOVA², A. VOROBEV¹†, A. MOJTABI³ AND B. ZAPPOLI⁴

¹Theoretical Physics Department, Perm State University, Perm, 614990, Russia

²Institute of Continuous Media Mechanics, Perm, 614013, Russia

³Institut de Mecanique des Fluides, Toulouse, 31062, France

⁴Centre National d'Etudes Spatiales, Toulouse, 31055, France

(Received 23 October 2003 and in revised form 6 March 2006)

A theoretical model describing the response of a single-phase near-critical fluid to small-amplitude, high-frequency translational vibrations is developed on the basis of the multiple-scale and averaging methods. Additionally to the usual terms of thermal convection, the equations and boundary conditions contain new terms responsible for the generation of pulsating and average flows due to vibrational forcing and fluid compressibility. The effect of compressibility is taken into account both in the boundary layers and in the bulk. A number of classical problems of convection and thermoacoustics are considered on the basis of the new model.

1. Introduction

High-frequency vibrations are known to generate average flows in non-homogeneously heated incompressible fluids (see Gershuni & Lyubimov 1998). The investigations of the influence of high-frequency vibrations on buoyancy convection started with the work of Zenkovskaya & Simonenko (1966), who developed an averaging technique in the framework of a Boussinesq approach. Later, the paper by Gershuni & Zhukhovitsky (1981) initiated a series of works on vibrational convection under weightlessness (see an extensive review in Gershuni & Lyubimov 1998). Most of these works were focused on situations when a container completely filled with a fluid undergoes periodic translational motion, i.e. does not change its orientation. In this case, called ‘uniform vibrations’ in Lyubimov (1995), a homogeneous fluid is quiescent in the reference frame of its container, and the pulsation velocity field is spatially uniform in the laboratory frame. The non-uniformity of the pulsation velocity field results from the density non-uniformity. If the density field is non-uniform due to non-isothermality, then the average ‘vibrational force’ turns out to be of second order with respect to the Boussinesq parameter, $\beta\theta$ (here β is the thermal expansion coefficient and θ is the scale of non-isothermality).

The situation is entirely different in cases when different parts of the fluid boundary move according to different laws. Examples are: non-translational vibrations of a container completely filled with a fluid, oscillations of a solid body immersed in a fluid, vibrations of a partially filled container, or vibrations of a set of immiscible

† Present address: The University of Michigan – Dearborn, Dearborn, MI 48128, USA.

fluids with a deformable interface boundary. In such conditions, called ‘non-uniform vibrations’ in Lyubimov (1995), the pulsation velocity field is spatially non-uniform even in a homogeneous fluid and the coupling of the non-uniformities of the pulsation velocity field with the non-uniform vorticity can generate an average flow. As shown by Lyubimov (1995), a Boussinesq approach becomes unreliable for the description of thermal vibrational convection under ‘non-uniform vibrations’. The averaged equations for arbitrary vibrations and the effective boundary conditions accounting for the generation of averaged fluid motion in viscous skin layers are obtained in Lyubimov (1995) and Gershuni & Lyubimov (1998). As a result of a separate analysis of the velocity distribution within a thin boundary layer (skin layer), the value of the velocity at the outer side of the boundary layer is obtained and applied as a boundary condition for the equations defining flows in the bulk (see Schlichting 1968).

Because of the significant compressibility of near-critical fluids, their convective stability cannot be characterized by the usual Rayleigh criterion. The investigations of thermal convection in compressible media started with Spiegel (1965), Polezhaev (1968), and Gitterman & Steinberg (1970). Chenoweth & Paolucci (1986) studied the convection of a general fluid taking into account arbitrary (not small) variations of density and fluid properties. The influence of vibrations on such systems was studied by Carles & Zappoli (1995) and Lyubimov (2000).

In compressible fluids, additional sources of motion under vibrations can originate in bulk phases via the bulk pressure gradient, thus provoking non-solenoidal motion in thermally homogeneous fluids. In hyper-compressible near-critical fluids, thermoacoustic coupling in the dissipative layers may change the bulk boundary conditions from those simply given by the presence of rigid walls, and also generate fluid motion. Carles & Zappoli (1995) and Jounet *et al.* (2000*a*) showed that extremely strong fluid expansion or contraction in thermal adaptation layers is able to generate significant boundary-layer-like flows. This changes the dynamic boundary conditions of the bulk momentum equation and may drastically modify the bulk flow structure. These thermomechanical couplings are due to the diverging compressibility of near-critical fluids and more generally to the critical anomalies of the transport parameters. These anomalies result in unexpected behaviour of near-critical fluids such as the existence of a fourth heat transfer mechanism of a thermoacoustic nature, named the piston effect, which allows heat to be transferred much faster than by diffusion or convection (see Boukari *et al.* 1990; Onuki, Hao & Ferrell 1990; Zappoli *et al.* 1990). The piston effect was recently shown to strongly influence the hydrodynamics of near-critical fluids (see Garrabos *et al.* 1998; Polezhaev, Emelianov & Gorbunov 1998).

In accordance with Zappoli & Carles (1996) this heat-transfer mechanism can be represented as the following sequence of processes:

- (i) Consider a near-critical fluid initially at rest. Instantaneously, one side of the container is heated; heat diffuses but only within a thin thermal boundary layer.
- (ii) Owing to hyper-compressibility, the heated boundary layer strongly expands and adiabatically compresses the bulk. This adiabatic compression results in the bulk warming up: the heat spreads into the bulk much faster than in the pure diffusive case.

It was later shown that the closer the state of a fluid to the critical point, the smaller the time needed for thermal equilibration. The typical time of the piston effect is determined by $\tau_{PE} \sim L^2/\gamma^2\chi$ (see Zappoli & Carles 1996), where $\gamma = c_p/c_V$ is the ratio between isobaric c_p and isochoric c_V heat capacities; γ becomes infinite approaching the critical point.

Although the direct numerical simulation of slowly time-dependent phenomena such as hydrodynamic stability or buoyant convection is possible, though difficult, the recent works of Jounet *et al.* (2000*a*) and Jounet, Zappoli & Mojtabi (2000*b*) on the response of near-critical fluids to vibrations showed the computational time to be extremely long and further studies on thermal vibrational convection in non-homogeneous near-critical fluids, like those conducted in ideal gases, to be impossible.

This is why, in the present paper, we derive a closed system of asymptotic equations with specific boundary conditions based on an averaging procedure which greatly decreases the computational time and allows an exploration of the response of thermally non-uniform nearly supercritical fluids to applied vibrations.

The action of translational vibrations on single-phase systems is considered. The equations obtained also account for buoyancy convection in a near-critical single-phase fluid and for interaction between the piston effect and convection mechanisms.

The paper is organized as follows. Section 2 presents the model and the governing equations, including the basic context of the motion of near-critical fluids subjected to vibrations, critical anomalies, hydrodynamics equations and the averaging method. The averaged equations and the effective boundary conditions describing thermal vibrational convection in a near-critical fluid subjected to non-uniform heating are derived in §3. It is shown in particular that a new source of flow motion appears in near-critical fluids, which originates from the thermoacoustic coupling enhanced by the diverging isothermal compressibility. This section also applies the average model to a set of classical physical situations and compares the results to those previously obtained. In §4 we discuss non-perfectly conducting walls and an acoustic filtering procedure. The main conclusions of the work are summarized in §5.

In Part 2 (Lyubimov *et al.* 2006) we assume that imposed temperature gradients (external heating) are small, so the effects of gravitational stratification and the generation of average temperature non-homogeneities by vibrations become significant. The new mathematical model of thermal vibrational convection is derived and discussed. In particular, special consideration is given to the case of isothermal boundary conditions and weightlessness, when the onset of convection is still possible due to vibrations.

2. Initial issues

2.1. Near-critical state

The transport properties of one-phase pure fluids in the vicinity of their liquid–gas critical point exhibit strong anomalies which can be expressed as a function of a parameter

$$\epsilon = (T_0 - T_c)/T_c, \quad (2.1)$$

where T_0 is a uniform background temperature and T_c is the critical temperature.

If a_T^2 , c^2 , β , c_p , c_V denote the square of the isothermal and adiabatic sound speeds, the thermal expansion coefficient, the isobaric and the isochoric heat capacity respectively, and κ , χ , η , ν are the thermal conductivity and diffusivity, and the dynamic and kinematic viscosity respectively, their near-critical behaviours can be expressed by the following asymptotes (see Stanley 1971):

$$a_T^2 \sim \epsilon^\gamma, \quad \beta, c_p \sim \epsilon^{-\gamma}; \quad c_V, c^2 \sim \epsilon^{-\alpha}; \quad \kappa \sim \epsilon^{-\Phi}, \quad \chi \sim \epsilon^{\gamma-\Phi}, \quad \eta, \nu \sim -\ln \epsilon. \quad (2.2)$$

Here $\gamma = 1.24$, $\alpha = 0.11$, $\Phi = 0.58$.

These expressions show that the singularities of isochoric capacity and isentropic speed of sound as well as the singularities of dynamic and kinematic viscosity are considerably weaker than the singularities of other quantities. This allows their singular behaviours to be neglected.

In this paper we assume a close proximity to the critical point. The series expansion of free energy about the critical point is used to derive the state equation and equation for the entropy. This expansion is known not to be applicable at the critical point itself and in its immediate proximity, since free energy is singular there. However this expansion can be used for the close, but not immediate, vicinity to the critical point where the effect of fluctuations becomes insignificant. In this range we are still able to use the hydrodynamic approach. We already need to take into account the divergence of isothermal compressibility, isobaric heat capacity, and heat conductivity; however, we do not need to consider the divergence of isochoric heat capacity, sound speed, and viscosity.

2.2. Basic equations

It is widely accepted that a near-critical fluid can be considered as a viscous, heat conducting and compressible Newtonian fluid and thus its motion is described by the Navier–Stokes equation. The temperature in the fluid can be obtained from the balance equation of any thermodynamic function. We use the entropy balance which contains the thermal and viscous dissipation as source terms, the latter being shown to be negligible. In order to relate pressure and entropy to the chosen independent thermodynamic variables, temperature and density, we need the equation of state $p = p(\rho, T)$ and the function $S = S(\rho, T)$ to be known as well. The van der Waals model gives correct phenomenological descriptions that, however, need to be refined when quantitative comparisons with experiments are needed (see Beysens & Garrabos 2001). The governing equations are thus

$$\rho \left(\frac{\partial \mathbf{v}}{\partial t} + (\mathbf{v} \cdot \nabla) \mathbf{v} \right) = -\nabla p + \eta \Delta \mathbf{v} + \rho \mathbf{g}, \quad (2.3a)$$

$$\rho T \left(\frac{\partial S}{\partial t} + (\mathbf{v} \cdot \nabla) S \right) = \kappa \Delta T, \quad \frac{\partial \rho}{\partial t} + \nabla \cdot (\rho \mathbf{v}) = 0; \quad (2.3b)$$

$$p = p(\rho, T), \quad S = S(\rho, T). \quad (2.3c)$$

Here the conventional notation is used. We have already neglected the viscous dissipation term and used the Stokes hypothesis in the momentum equation (the term proportional to $\nabla(\nabla \cdot \mathbf{v})$ is omitted). Owing to compressibility, $\nabla \cdot \mathbf{v}$ can be non-zero, but remains small. As our purpose is to obtain the asymptotic equations, which should not contain any small terms, only the main ones, we omit this part of the dissipative term. As only small deviations from the initial near-critical state are addressed, we replace the transport parameters by their values in the initial state, since their variation leads to negligible higher-order corrections.

These equations must be completed with the initial and boundary conditions. Also, the vibrational influence is contained in the boundary conditions.

We consider the influence of uniform vibrations, which implies that the pulsation velocity of a fluid \mathbf{w} is constant as a function of space at leading order, i.e. $\mathbf{w}_0 = \text{constant}(\mathbf{r})$. This constant vector is determined by the applied vibrational forcing. Such vibrations are realized by translational movements of a container completely filled with fluid and oscillating under the law $a \mathbf{j} \sin(\omega t)$, where \mathbf{j} is the unit vector defining the direction of vibration, and a, ω are the amplitude and



FIGURE 1. Working temperature range. Here the constant background temperature, $T_0 = T_c(1 + \epsilon)$, and variations in temperature examined start from the second order of ϵ : $T'/T_c = \epsilon^2 T_2 + \epsilon^3 T_3 + \dots$

frequency of vibrations. The pulsation velocity of a fluid at leading order is then also determined by vector \mathbf{j} , namely $\mathbf{w}_0 = a\omega \mathbf{j} \cos(\omega t)$. Several mechanisms (temperature non-homogeneities for instance) induce the small non-homogeneities in pulsation velocity, and these non-homogeneities result in average motion.

Below, to derive the governing equations and effective boundary conditions, we will use the reference frame attached to the vibrating container. The zeroth order of the fluid pulsational velocity is eliminated in this case, and w_0 denotes the vibrational velocity of the container. The next orders, w_1, w_2 , etc., describe the non-homogeneities of the pulsational field of the fluid.

We assume that the constant background temperature T_0 exceeds the critical point T_c , and that the difference $(T_0 - T_c)$ is a quantity of the first order of smallness, $T_0 - T_c = \epsilon T_c > 0$. In this paper, the temperature difference between boundaries (imposed external heating) is of the second order in ϵ , $\theta = O(\epsilon^2)$ (θ is a typical scale of heating in T_c units). These two assumptions allow us to avoid phase transitions, since they guarantee $T > T_c$. Smaller temperature differences and isothermal boundary conditions will be considered in Part 2 (Lyubimov *et al.* 2006).

The temperature distribution is presented as a sum: $T = T_0 + T'$, where T' is the deviation from the background value T_0 . Since only single-phase systems are considered (the temperature exceeds the critical value), the following inequality holds: $|T'| \ll (T_0 - T_c)$. By presenting T' in the form of a series of the small parameter ϵ , for the relative deviation of temperature from the critical value we have

$$\frac{T - T_c}{T_c} = \frac{T_0 - T_c}{T_c} + \frac{T'}{T_c} = \epsilon T_1 + \epsilon^2 T_2 + \epsilon^3 T_3 + \dots \tag{2.4}$$

where T_1, T_2, T_3, \dots are generally functions of space and time. The first term in the temperature expansion represents the reference background point. This background temperature is assumed to be constant and we take $T_1 = 1$. The deviations from this temperature are assumed to be small, and a non-constant deviation term appears for the first time in the second-order term $\epsilon^2 T_2$. The case considered is illustrated by figure 1.

The deviations of temperature from the background state cannot be taken to be of the same order as the difference in temperature from the critical point. This would change the problem completely. With our present assumptions we can automatically guarantee that the system does not go beyond the critical point in its evolution. In other words, we study fluid motion, convection, on some specific but steady background. Thus we can use asymptotical analysis (expansion in series of a small parameter). The model allowing temperature deviations at the first (and not the second) order is physically real and possible. However, this model assumes that, virtually, there is no background state, and the system might go beyond the critical point (the second phase might appear), which multiplies the complexity significantly.

The density is chosen as the second independent thermodynamic variable. Variations of density can be caused by temperature changes (due to thermal expansion) and by pressure changes in a cavity (due to mechanical, isothermal compressibility). Near the critical point, the coefficients of both thermal expansion and isothermal compressibility exhibit singular behaviour. That is why relative density changes may greatly exceed relative temperature variations. The order of magnitude of density changes is determined from the solution of a particular problem. Here we just assume that the density variations are much smaller than ρ_c , and represent them as a similar series of the parameter ϵ :

$$\frac{\rho - \rho_c}{\rho_c} = \epsilon \rho_1 + \epsilon^2 \rho_2 + \dots \quad (2.5)$$

Let us emphasize that this expansion is general. Further study should show which terms in the expansions differ from zero. Moreover this might be different for the boundary layer and bulk, for the pulsational and average components.

Further theory is based on expansions of all unknown variables in similar series of ϵ .

2.3. Averaging procedure

The initial equations (2.3) can be substantially simplified if we take advantage of some important differences in the typical time and space scales.

We assume that the frequency of vibrations ω is so high that the boundary layer thicknesses ($\delta_v = \sqrt{\nu/2\omega}$ and $\delta_\chi = \sqrt{\chi/2\omega}$) are small in comparison with a typical length L : $\delta \ll L$; at the same time, it is so small that the wavelength of sound λ exceeds L considerably: $L \ll \lambda$. These assumptions enable us to consider hydrodynamic fields in the bulk and in the boundary layer separately. The solution of the second problem gives the effective boundary conditions for the first one. Additionally, the amplitude of vibrations a is assumed to be small: $a \ll L$. This allows us to neglect nonlinear terms in the equations for pulsations.

Amongst the time scales, we can single out a vibration period ($1/\omega$) and dissipative times ($\tau_\chi = L^2/\chi$, $\tau_v = L^2/\nu$). For practical use, the behaviour of a convective system on time scales higher than the vibration period needs to be known. The averaging description enables us to decompose the system of equations into two: for average and pulsating fields. To do that we represent all physical fields F as a sum of average \bar{F} and pulsating \tilde{F} components: $F(\mathbf{r}, t) = \bar{F}(\mathbf{r}, t) + \tilde{F}(\mathbf{r}, \omega t)$. For average and pulsating components of the velocity we use different notation, namely $\mathbf{v}(\mathbf{r}, t) = \mathbf{u}(\mathbf{r}, t) + \mathbf{w}(\mathbf{r}, \omega t)$.

The averaging procedure is the simplest for harmonic vibrations, when $\tilde{F}(\mathbf{r}, \omega t) = f(\mathbf{r}) \cos(\omega t)$. In addition, this is the most important case. For such vibrations:

$$\overline{\bar{F}} = \bar{F}, \quad \overline{\tilde{F}} = 0, \quad \overline{\tilde{F}\bar{F}} = 0, \quad \overline{\frac{\partial}{\partial t}(\dots)} = 0. \quad (2.6)$$

The above expression also gives the following useful result:

$$\overline{\tilde{F}_1 \frac{\partial \tilde{F}_2}{\partial t}} = -\overline{\tilde{F}_2 \frac{\partial \tilde{F}_1}{\partial t}}. \quad (2.7)$$

It should be noted that the vibration period and the typical time scale of the piston effect are related through $\omega \tau_{PE} \sim (L/\gamma \delta_\chi)^2$ (where $\gamma = c_p/c_v$ is the specific-heat ratio). This combination is assumed finite. This is an arbitrary choice; to analyse the influence of the piston effect we need to assume that the vibration period is of the same order

as the time scale of the piston effect; later equations will contain several terms determined by this ratio.

Expressions (2.6) and (2.7) are used to average the equations. Equations determining the pulsational fields are obtained by subtracting the average part from the whole ones.

Finally, let us summarize the algorithm used for derivation of the averaged models. The algorithm is based on the multiple-scale method and averaging procedure.

(i) In the first step we expand all variables (plus time and spatial coordinate when the boundary layer is considered) in series of the small parameter ϵ . We also choose the relations between other dimensionless parameters and ϵ . Then we substitute the expansions into the basic equations (2.3) and collect the terms of the same order of ϵ , writing the different orders of the equations separately.

(ii) The second step is averaging the equations. All variables are divided into average and pulsation parts, and the equations are averaged using (2.6)–(2.7). Thus, the average and pulsation parts of the equations are separated.

(iii) In the third step we analyse the equations obtained. These equations must satisfy several requirements: the set of equations must be closed; the equations may not contain unknown variables from the equations of higher orders. The pulsation equations must be linear. The average equations must describe the convection-like motion; they must contain the non-steady and nonlinear terms, as well as the viscous and heat-conductive diffusion terms. The expansion should be cut off when the average equations already include these terms.

(iv) If the resulting equations are unclosed or do not satisfy other requirement listed, it is necessary to choose different initial expansions or relations, returning to the first step. The requirement that the governing equations must be closed is the main condition for the relations between the dimensionless parameters.

This algorithm is applied to construct all the averaged models of this work (both here and in Part 2). It is used both for the derivation of the bulk equations and for the derivation of the effective boundary conditions.

3. Derivation of averaged equations

3.1. *The bulk*

Let us take the reference frame of a vibrating container, i.e. moving with a velocity \mathbf{w}_0 . Equations (2.3) are non-dimensionalized as follows:

$$\rho \rightarrow \rho_0(1 + \rho), \quad T \rightarrow T_0(1 + T), \quad p \rightarrow p_0(1 + p), \quad S \rightarrow c_V(1 + S); \quad (3.1a)$$

$$\mathbf{v} \rightarrow (a\omega)\mathbf{v}, \quad \mathbf{w}_0 \rightarrow (a\omega)\mathbf{w}_0, \quad t \rightarrow \frac{1}{\omega}t, \quad \mathbf{g} \rightarrow -g\boldsymbol{\gamma}. \quad (3.1b)$$

As a result, one obtains the following dimensionless equations:

$$(1 + \rho) \left[\frac{\partial \mathbf{v}}{\partial t} + \mu (\mathbf{v} \cdot \nabla) \mathbf{v} \right] = -\frac{1}{\mu A} \nabla p + \epsilon_\eta^2 \Delta \mathbf{v} - \alpha(1 + \rho)\boldsymbol{\gamma} - (1 + \rho) \frac{\partial \mathbf{w}_0}{\partial t}, \quad (3.2a)$$

$$(1 + \rho)(1 + T) \left[\frac{\partial S}{\partial t} + \mu (\mathbf{v} \cdot \nabla) S \right] = \epsilon_\kappa^2 \Delta T, \quad (3.2b)$$

$$\frac{\partial \rho}{\partial t} + \mu \nabla \cdot ((1 + \rho)\mathbf{v}) = 0. \quad (3.2c)$$

These equations are completed with the equations of state: $p = p(\rho, T)$ and $S = S(\rho, T)$, which are expanded in series of small independent quantities (ρ, T) :

$$p = p_\rho \rho + p_T T + \frac{1}{2}(p_{\rho\rho} \rho^2 + 2p_{\rho T} \rho T + p_{TT} T^2) + \dots, \quad (3.3a)$$

$$S = S_\rho \rho + S_T T + \frac{1}{2}(S_{\rho\rho} \rho^2 + 2S_{\rho T} \rho T + S_{TT} T^2) + \dots. \quad (3.3b)$$

Hereinafter we use the conventional notations for thermodynamic derivatives,

$$p_\rho = \left(\frac{\partial p}{\partial \rho} \right)_T, \quad S_\rho = \left(\frac{\partial S}{\partial \rho} \right)_T, \quad p_T = \left(\frac{\partial p}{\partial T} \right)_\rho, \quad p_{\rho T} = \frac{\partial^2 p}{\partial \rho \partial T} \dots. \quad (3.4)$$

In equations (3.2) the following dimensionless parameters are introduced:

$$\mu = \frac{a}{L}, \quad A = \frac{(\omega L)^2}{p_c / \rho_c}, \quad \alpha = \frac{g}{a \omega^2}, \quad \epsilon_\eta^2 = \frac{\eta}{\rho_c \omega L^2}, \quad \epsilon_\kappa^2 = \frac{\kappa}{\rho_c \omega L^2 c_V} \quad (3.5)$$

– the amplitude of vibrations (μ), the square of the sound wavelength (A), parameter α that characterizes the gravity level and two parameters characterizing the thicknesses of the skin layers (ϵ_η^2 for the viscous and ϵ_κ^2 for the thermal layer).

Let us expand all variables in series of the small parameter ϵ :

$$T = \epsilon + \epsilon^2 T_2 + \epsilon^3 T_3 + \dots, \quad p = \epsilon p_1 + \epsilon^2 p_2 + \epsilon^3 p_3 + \dots, \quad (3.6a)$$

$$\rho = \epsilon \rho_1 + \epsilon^2 \rho_2 + \dots, \quad S = \epsilon S_1 + \epsilon^2 S_2 + \dots, \quad \mathbf{v} = \epsilon \mathbf{v}_1 + \epsilon^2 \mathbf{v}_2 + \dots. \quad (3.6b)$$

Using the definition of the critical point, one immediately finds $p_1 = p_T \equiv (\partial p / \partial T)_\rho$.

The amplitude of vibrations is assumed to be small in comparison with the size of the container, i.e. $\mu \ll 1$. This assumption allows us to neglect the nonlinear terms in the equations for pulsations.

The limiting case of high-frequency vibrations, which implies that the period of vibrations is small in comparison with the viscous and thermal dissipative time scales, is considered:

$$\frac{1}{\omega} \ll \frac{L^2}{\eta / \rho_c}, \quad \frac{1}{\omega} \ll \frac{L^2}{\kappa / (\rho_c c_V)}. \quad (3.7)$$

That is, the parameters ϵ_η^2 and ϵ_κ^2 are small. These two inequalities make the dissipative effects for pulsations important only in thin boundary layers near the rigid walls of the container. As a result, we can neglect the dissipative terms in the equations for pulsations in the bulk.

We also suppose that the sound wavelength for the vibration frequency is large compared to the container size:

$$\frac{c}{\omega} = \frac{\sqrt{p_c / \rho_c}}{\omega} \gg L, \quad \text{or} \quad A \equiv \frac{(\omega L)^2}{p_c / \rho_c} \ll 1. \quad (3.8)$$

The inequalities (3.7) and (3.8) impose the limitations on the vibration frequency from below and above respectively. These inequalities are compatible if the restriction

$$c \gg \frac{\eta / \rho_c}{L} \quad (3.9)$$

and the similar restriction for thermal diffusivity are satisfied. These two restrictions are independent of the vibration parameters.

The inequalities (3.7)–(3.8) may fail in the immediate proximity of the critical point, which, in any case, is beyond our consideration. Nevertheless, they are safely satisfied in the close but not immediate proximity of the critical point, the parameter range we are interested in.

Thus, we assume

$$\mu \ll 1, \quad A \ll 1, \quad \epsilon_\eta^2 \ll 1, \quad \epsilon_\kappa^2 \ll 1. \quad (3.10)$$

Finally, we conclude that the problem under consideration includes the following small parameters: $\epsilon, \mu, A, \epsilon_\eta^2, \epsilon_\kappa^2$.

The scaling laws (2.2) define the relationship between the parameters ϵ_η^2 and ϵ_κ^2 , namely

$$\epsilon_\eta^2 \ll \epsilon_\kappa^2, \quad (3.11)$$

since divergence of the thermal conductivity, κ , is much stronger than the weak divergence of c_V and η .

The relations between other small parameters remain arbitrary. It is convenient, however, to impose formal relations between them. The choice of these formal relations is restrained only by the requirement of accounting for different physical effects at the same orders of expansion. We impose the following relationships:

$$\mu \sim \epsilon, \quad A \sim \epsilon, \quad \epsilon_\eta^2 \sim \epsilon^2, \quad \epsilon_\kappa^2 \sim \epsilon, \quad \alpha \sim \epsilon^2. \quad (3.12)$$

Tentative calculations have shown that any other choice results in the loss of some effects, or even in failure to obtain a closed system of equations.

The effective decomposition of variables into pulsating and average components is possible only when the amplitude of vibration is small compared to the typical length scale. In this case, the volumetric vibrational mechanism makes a large contribution only if the vibrational accelerations are large compared to the static gravity. That is why the parameter $\alpha = g/(a\omega^2)$ was assumed to be small. If we took the second order of smallness for α , then the gravitational effects arise at the same order as the volumetric vibrational effects. Note that the parameter α was also considered as a small quantity when average equations for the description of thermal convection in incompressible fluid subjected to uniform vibrations were derived (see Zenkovskaya & Simonenko 1966). If vibrational accelerations are not strong, the volumetric vibrational mechanism makes just a small contribution. However, the volumetric vibrational effects predominate under microgravity conditions. Additionally, in the case of a compressible fluid, vibrations generate strong flows in the boundary layers, which exert a strong influence on the bulk flow.

In accordance with the main idea of the multiple-scale method, the time derivative must be represented as a sum:

$$\frac{\partial}{\partial t} = \frac{\partial}{\partial t_0} + \epsilon^2 \frac{\partial}{\partial t_2}. \quad (3.13)$$

Here t_0 corresponds to quickly varying, pulsating processes; t_2 describes slowly varying, average motion. The quantities corresponding to the vibrational forcing, for instance w_0 , are functions of t_0 only.

It turns out that, to obtain the final averaged equations, only these two terms are needed. The absence of the term $\epsilon \partial/\partial t_1$ in the expansion is related to the fact that slow time describes the relaxation processes due to the viscous dissipation and therefore should appear at the same order of the expansion as the viscous term (see Gershuni & Lyubimov 1998).

Let us examine the expressions appearing at different orders of the expansion. In the leading (zeroth for (3.2a) and first for (3.2b, c)) order, we obtain

$$\frac{\partial w_0}{\partial t_0} = -\frac{1}{\mu A} \nabla p_2, \quad p_2 = p_T T_2 + p_{\rho T} \rho_1; \quad \frac{\partial \rho_1}{\partial t_0} = \frac{\partial S_1}{\partial t_0} = 0. \quad (3.14)$$

Recall that the overbar is used to designate the average components, and the tilde designates the pulsating ones. A variable without a bar or tilde means the sum of the two components (the whole variable). Additionally, we see from (3.14) that ρ_1 and S_1 do not have pulsating parts, so we omit the overbar for their notation later on.

The next (first for (3.2a) and second for (3.2b, c)) order of equations gives

$$\frac{\partial \mathbf{v}_1}{\partial t_0} = -\frac{1}{\mu A} \nabla p_3 - \rho_1 \frac{\partial \mathbf{w}_0}{\partial t_0}, \quad \tilde{p}_3 = p_T \tilde{T}_3 + p_{\rho T} \rho_1 \tilde{T}_2, \quad (3.15a)$$

$$\frac{\partial S_2}{\partial t_0} = 0, \quad \tilde{S}_2 = S_\rho \tilde{\rho}_2 + S_T \tilde{T}_2, \quad \frac{\partial \rho_2}{\partial t_0} + \mu \nabla \cdot \mathbf{v}_1 = 0. \quad (3.15b)$$

Here the first and the last equations contain both average and pulsation components, which we divide later. At the next order, only the energy equation (3.2a) is needed:

$$\frac{\partial S_3}{\partial t_0} + \frac{\partial S_1}{\partial t_2} + \mu (\mathbf{v}_1 \cdot \nabla) S_1 = \epsilon_\kappa^2 \Delta T_2, \quad (3.16a)$$

$$S_1 = S_\rho \rho_1, \quad S_3 = S_\rho \rho_3 + S_T T_3 + S_{\rho\rho} \rho_1 \rho_2 + S_{\rho T} \rho_1 T_2. \quad (3.16b)$$

The second order of the momentum equation (3.2) gives the corrections to the pulsation velocity, which we are not interested in. Only the third order of this equation needs to be written down:

$$\frac{\partial \mathbf{v}_3}{\partial t_0} + \frac{\partial \mathbf{v}_1}{\partial t_2} + \mu (\mathbf{v}_1 \cdot \nabla) \mathbf{v}_1 + \rho_1 \frac{\partial \mathbf{v}_2}{\partial t_0} + \rho_2 \frac{\partial \mathbf{v}_1}{\partial t_0} = -\frac{1}{\mu A} \nabla p_5 + \epsilon_\eta^2 \Delta \mathbf{v}_1 - \alpha \rho_1 \boldsymbol{\gamma} - \rho_3 \frac{\partial \mathbf{w}_0}{\partial t_0}. \quad (3.17)$$

Equations (3.15)–(3.17) are again written both for the pulsation and averaged components.

Now, let us separate the average and pulsation parts of the equations. Based on (3.14), (3.15), for the pulsating variables we obtain

$$\tilde{T}_2 = -\frac{\mu A}{p_T} \frac{\partial \Phi}{\partial t_0}, \quad \tilde{\rho}_2 = -\frac{S_T}{S_\rho} \tilde{T}_2; \quad (3.18a)$$

$$\nabla \cdot \mathbf{w}_1 = -A \frac{S_T}{p_T S_\rho} \frac{\partial^2 \Phi}{\partial t_0^2}, \quad \nabla \times \mathbf{w}_1 = \mathbf{w}_0 \times \nabla \rho_1; \quad (3.18b)$$

$$\nabla \tilde{T}_3 = -\frac{\mu A}{p_T} \frac{\partial}{\partial t_0} (\mathbf{w}_1 + \rho_0 \mathbf{w}_0) - \frac{p_{\rho T}}{\partial T} \nabla \rho_1 \tilde{T}_2, \quad (3.18c)$$

where Φ is the pulsating velocity potential, $\mathbf{w}_0 = \nabla \Phi$ (for translational vibrations $\Phi = (\mathbf{w}_0 \cdot \mathbf{r})$, where \mathbf{r} is the radius vector). The reference point for the potential is discussed below in §3.3.

By averaging (3.16), (3.17), the following equations for the average flow are derived for the case of harmonic vibrations with uniform phase:

$$\begin{aligned} \frac{\partial \mathbf{u}_1}{\partial t_2} + \mu (\mathbf{u}_1 \cdot \nabla) \mathbf{u}_1 = & -\nabla \Pi + \epsilon_\eta^2 \Delta \mathbf{u}_1 - \alpha \rho_1 \boldsymbol{\gamma} - \mu (\mathbf{w}_1 \cdot \mathbf{w}_0) \nabla \rho_1 \\ & + \frac{1}{2} \mu A \frac{S_T}{p_T S_\rho} \left(1 + \frac{p_{\rho T}}{p_T} + \frac{S_{\rho\rho}}{S_\rho} - \frac{S_{\rho T}}{S_T} \right) \Phi^2 \nabla \rho_1, \end{aligned} \quad (3.19a)$$

$$\frac{\partial \rho_1}{\partial t_2} + \mu (\mathbf{u}_1 \cdot \nabla) \rho_1 = -\epsilon_\kappa^2 \frac{p_{\rho T}}{S_\rho p_T} \Delta \rho_1, \quad (3.19b)$$

$$\nabla \cdot \mathbf{u}_1 = 0. \quad (3.19c)$$

Here all gradient terms are included in the term $-\nabla \Pi$, and the pulsating variables correspond only to amplitudes of the whole quantities (the same notation is kept): $(\mathbf{w}_1, \mathbf{w}_0, \Phi) \rightarrow (\mathbf{w}_1, \mathbf{w}_0, \Phi) \cos(\omega t)$.

3.2. Derivation of effective boundary conditions

The case of rigid, perfectly conducting boundaries is considered. To examine the fluid behaviour inside the skin layer we use a coordinate system where z indicates the coordinate normal to the wall, and x and y are the tangential coordinates. Velocity is represented as $\mathbf{v} = (\mathbf{V}, v_z)$, where \mathbf{V} , v_z indicate the tangential and normal components respectively, and similarly for the pulsating velocity $\mathbf{w}_0 = (\mathbf{W}_0, w_{0z})$ and for the differentiation operator $\nabla = (\nabla_2, \partial/\partial z)$.

The consideration starts with equations

$$(1 + \rho) \left[\frac{\partial \mathbf{V}}{\partial t} + \mu \left((\mathbf{V} \cdot \nabla_2) \mathbf{V} + v_z \frac{\partial \mathbf{V}}{\partial z} \right) \right] = -\frac{1}{\mu A} \nabla_2 p + \epsilon_\eta^2 \frac{\partial^2 \mathbf{V}}{\partial z^2} - (1 + \rho) \frac{\partial \mathbf{W}_0}{\partial t_0}, \quad (3.20a)$$

$$(1 + \rho) \left[\frac{\partial v_z}{\partial t} + \mu \left((\mathbf{V} \cdot \nabla_2) v_z + v_z \frac{\partial v_z}{\partial z} \right) \right] = -\frac{1}{\mu A} \frac{\partial p}{\partial z} + \epsilon_\eta^2 \frac{\partial^2 v_z}{\partial z^2} - \alpha(1 + \rho) - (1 + \rho) \frac{\partial w_{0z}}{\partial t_0}, \quad (3.20b)$$

$$(1 + \rho)(1 + T) \left[\frac{\partial S}{\partial t} + \mu \left((\mathbf{V} \cdot \nabla_2) S + v_z \frac{\partial S}{\partial z} \right) \right] = \epsilon_\kappa^2 \frac{\partial^2 T}{\partial z^2}, \quad (3.20c)$$

$$\frac{\partial \rho}{\partial t} + \mu \left[\nabla_2 \cdot ((1 + \rho)\mathbf{V}) + \frac{\partial}{\partial z} ((1 + \rho)v_z) \right] = 0. \quad (3.20d)$$

Only the terms with any influence on the further analysis are kept here (these are equations (3.2) with divided tangential and normal components).

We impose the following boundary conditions at the wall:

$$z = 0: \quad \mathbf{v} = 0, \quad T = T_B. \quad (3.21)$$

All variables must match their bulk values at the outer edge of the skin layer.

Near the boundary, in pulsating flow, the viscous and thermal boundary layers are formed. In our approximation, the thicknesses of the skin layers (δ_v , δ_χ) are much smaller than the typical length L . That is why the boundary conditions have to be set at the outer edges of the skin layers. First, we find the distributions of physical quantities inside the boundary layers, and then the limit of zero thickness of the skin layer is taken to derive the necessary effective boundary conditions.

For the skin-layer analysis, we assume that the derivative along the normal coordinate is represented by the series

$$\frac{\partial}{\partial z} = \epsilon^{-1} \frac{\partial}{\partial z_{-1}} + \frac{\partial}{\partial z_0} + \dots \quad (3.22)$$

The leading (minus-first for (3.20b) and zeroth for (3.20c,d)) order of the series expansion is

$$\frac{\partial p_2}{\partial z_{-1}} = 0, \quad p_2 = p_T T_2 + p_{\rho T} \rho_1, \quad (3.23a)$$

$$\frac{\partial S_1}{\partial t_0} = \epsilon_\kappa^2 \frac{\partial^2 T_2}{\partial z_{-1}^2}, \quad \frac{\partial \rho_1}{\partial t_0} + \mu \frac{\partial v_{z1}}{\partial z_{-1}} = 0, \quad S_1 = S_\rho \rho_1. \quad (3.23b)$$

Like the derivation of the equations for the bulk, (3.23) contain both pulsating and averaged variables, which can be divided by averaging (which is simple here since these equations are linear).

In the case of harmonic vibrations, the solution of equations (3.23b) for the pulsational component of the velocity, satisfying the boundary conditions on the rigid

wall, is

$$w_{1z} = \text{Re} \left[-\frac{1-i}{\sqrt{2}} (1 - \exp(-\beta z)) \frac{A\epsilon_\kappa}{\sqrt{-p_{\rho T} S_\rho p_T}} \Phi \exp(it) \right], \quad \left. \begin{aligned} & \\ & \beta = \frac{1+i}{\sqrt{2}} \frac{1}{\epsilon_\kappa} \sqrt{-\frac{p_{\rho T}}{S_\rho p_T}}. \end{aligned} \right\} \quad (3.24)$$

In the limit of $\beta z \rightarrow \infty$ we obtain the effective boundary condition for the pulsating field in the form

$$w_{1z} = \text{Re} \left[-\frac{1-i}{\sqrt{2}} \frac{A\epsilon_\kappa}{\sqrt{-p_{\rho T} S_\rho p_T}} \Phi \exp(it) \right]. \quad (3.25)$$

Thus, the boundary condition for the pulsating velocity differs from the trivial impermeability condition. The essential requirement is perfect thermal conductivity of the boundary (temperature of the wall is fixed). This effect does not occur for adiabatic boundaries. We do not need to implement any conditions for the tangential components of the pulsating velocity field, since it is described by inviscid equations in the bulk.

Equations (3.23) give the trivial conditions for the normal component of the average velocity and for the average temperature field: $u_{1z} = 0, T_2 = T_B$. To obtain the effective boundary condition for the tangential velocity component, it is necessary to examine the next order of the expansion (zeroth for (3.20*b*) and first for (3.20*a*)):

$$\frac{1}{\mu A} \left[\frac{\partial p_3}{\partial z_{-1}} + \frac{\partial p_2}{\partial z_0} \right] + \frac{\partial w_{0z}}{\partial t_0} = 0, \quad \frac{\partial \mathbf{V}_1}{\partial t_0} = -\frac{1}{\mu A} \nabla p_3 + \epsilon_\eta^2 \frac{\partial^2 \mathbf{V}_1}{\partial z_{-1}^2} - \rho_1 \frac{\partial \mathbf{W}_0}{\partial t_0}. \quad (3.26)$$

By averaging these equations, one obtains the trivial no-slip condition for the tangential component of average velocity: $\bar{\mathbf{V}}_1 = \mathbf{u}_{1\tau} = 0$.

3.3. Final governing equations

The right-hand sides of equations (3.18*b*) for the first order of the pulsation velocity are periodic in time and develop with no phase difference with respect to the vibrational forcing, whereas boundary condition (3.25) includes the phase shift. That means that the pulsation field in the bulk oscillates with some shift in phase with respect to the vibrations applied. Nevertheless, the corresponding, shifted, part of the pulsation field (proportional to $\sin(\omega t)$ if the applied forcing is determined by $\cos(\omega t)$) satisfies the homogeneous equations, and thus, is vortex-free. Such terms in the averaged momentum equation lead to gradient effects. Their influence has been included in the term with modified pressure Π ; and they are not essential for the current consideration. Below, we will consider only that part of the pulsation velocity which oscillates with the same phase as the forcing, and the amplitude of this velocity will be denoted as \mathbf{w}_1 .

We rewrite the equations for this quantity in dimensional form, namely, using (3.18*b*),

$$\nabla \times \mathbf{w}_1 = \beta \nabla T \times \mathbf{w}_0, \quad \nabla \cdot \mathbf{w}_1 = -\left(\frac{\omega}{c}\right)^2 \Phi, \quad \nabla \Phi = \mathbf{w}_0. \quad (3.27)$$

The boundary condition comes from (3.25):

$$w_{1n} = \left(\frac{\omega}{c}\right)^2 \gamma \delta_\chi \Phi. \quad (3.28)$$

Next, we rewrite the equation for the energy balance (3.19*b*) in its generally recognized form over temperature variations. The average part of equations (3.14) has the form:

$$\nabla \bar{p}_2 = p_T \nabla \bar{T}_2 + p_{\rho T} \nabla \rho_1 = 0. \quad (3.29)$$

Integrating this equation with respect to the coordinates and applying the well-known formula, $\beta = p_\rho / (\rho p_T)$, one derives the following state equation:

$$\rho_1 = \rho_0(t) - \beta \rho_c \bar{T}_2, \quad (3.30)$$

where $\rho_0(t)$ is independent of the coordinates. By integrating (3.30) over the volume of the container, we obtain

$$\rho_0(t) = \frac{1}{V} \int_V \rho_1 \, dV + \rho_c \beta \frac{1}{V} \int_V T_2 \, dV. \quad (3.31)$$

Since the whole fluid mass is fixed, from (3.31) we derive

$$\frac{\partial \rho_1}{\partial t_2} = \beta \rho_c \frac{\partial}{\partial t_2} (\bar{T}_2 - \langle \bar{T}_2 \rangle), \quad (3.32)$$

where $\langle T \rangle = (1/V) \int_V T \, dV$. The term containing $\langle T \rangle$ describes the effects of pressure changes inside the considered volume (thermodynamic part of pressure, see §4.2).

Substitution of (3.30) and (3.31) into (3.19b) allows us to obtain the following heat balance equation (in dimensional form):

$$\frac{\partial T_2}{\partial t} + (\mathbf{u}_1 \cdot \nabla) T_2 = \chi \Delta T_2 + \frac{\partial}{\partial t} \langle T_2 \rangle. \quad (3.33)$$

Introducing the new notation σ for the combination of the second derivatives of thermodynamic quantities:

$$\sigma = \rho_c \left(2 \frac{p_{\rho T}}{p_T} - \frac{S_{\rho T}}{S_T} \right); \quad p_T \equiv \left(\frac{\partial p}{\partial T} \right)_\rho, \quad p_{\rho T} \equiv \frac{\partial^2 p}{\partial \rho \partial T}, \dots, \quad (3.34)$$

and using the thermodynamic equality, $S_{\rho\rho}/S_\rho = -2/\rho_c + p_{\rho T}/\rho_T$, we rewrite equation (3.19a) as follows (in dimensional form):

$$\begin{aligned} \frac{\partial \mathbf{u}_1}{\partial t} + (\mathbf{u}_1 \cdot \nabla) \mathbf{u}_1 = & -\nabla \Pi + \nu \Delta \mathbf{u}_1 + g\beta T_2 \boldsymbol{\gamma} + \frac{1}{2} (\mathbf{w}_1 \cdot \mathbf{w}_0) \beta \nabla T_2 \\ & + \frac{\sigma - 1}{4} \left(\frac{\omega}{c} \right)^2 \Phi^2 \beta \nabla T_2. \end{aligned} \quad (3.35)$$

Note that the dimensionless parameter σ is determined only by the properties of the fluid. For an ideal gas $\sigma = 2$ and for van der Waals model $\sigma = 3$.

Finally in dimensional form (omitting indices), the governing equations for average flows are

$$\frac{\partial \mathbf{u}}{\partial t} + (\mathbf{u} \cdot \nabla) \mathbf{u} = -\nabla \Pi + \nu \Delta \mathbf{u} + g\beta T \boldsymbol{\gamma} + \frac{1}{2} (\mathbf{w} \cdot \mathbf{w}_0) \beta \nabla T + \frac{\sigma - 1}{4} \left(\frac{\omega}{c} \right)^2 \Phi^2 \beta \nabla T, \quad (3.36a)$$

$$\nabla \cdot \mathbf{u} = 0, \quad (3.36b)$$

$$\frac{\partial T}{\partial t} + (\mathbf{u} \cdot \nabla) T = \chi \Delta T + \frac{\partial}{\partial t} \langle T \rangle, \quad \langle T \rangle = \frac{1}{V} \int_V T \, dV; \quad (3.36c)$$

and the problem for pulsating flows is

$$\nabla \times \mathbf{w} = \beta \nabla T \times \mathbf{w}_0, \quad \nabla \cdot \mathbf{w} = - \left(\frac{\omega}{c} \right)^2 \Phi; \quad \nabla \Phi = \mathbf{w}_0. \quad (3.37)$$

Here \mathbf{w}_0 is the pulsational velocity of the container. The effective boundary conditions

(for rigid, perfectly conducting walls) are

$$T = T_B, \quad \mathbf{u} = 0, \quad w_n = \left(\frac{\omega}{c}\right)^2 \gamma \delta_\chi \Phi, \tag{3.38}$$

where T_B is the wall temperature (it may depend on time and/or coordinates).

Let us determine the reference point of the potential Φ . To this end, we will use the fact that the whole mass of a fluid is fixed,

$$\frac{\partial}{\partial t_0} \int_V \rho \, dV = 0. \tag{3.39}$$

It is convenient to divide the integral over the total constant volume of the container V into a sum of two integrals: over the volume occupied by the boundary layers near the solid walls $V - V_0$, and over the bulk volume V_0 . In these integrals we should take into account that ρ_1 is independent of t_0 in the bulk, and is a function of t_0 within the boundary layers. Keeping the leading terms of the density expansions in both integrals, one obtains the relation

$$\frac{\partial}{\partial t_0} \int_V \rho \, dV = \int_{V-V_0} \frac{\partial \rho_1}{\partial t_0} \, dV + \epsilon \int_{V_0} \frac{\partial \rho_2}{\partial t_0} \, dV = 0. \tag{3.40}$$

Using the formulae (3.23b), (3.25), and (3.18a), we obtain the final expression for Φ :

$$\int_V \Phi \, dV + \gamma \delta_\chi \oint_S \Phi \, dS = 0. \tag{3.41}$$

Here S is the surface of the container, and expression (3.41) is written in its dimensional form.

Having analysed the equations for the average hydrodynamic fields (3.36), one sees that, in addition to the usual buoyancy ($g\beta T\gamma$) and vibration ($(\mathbf{w} \cdot \mathbf{w}_0)\beta\nabla T/2$) forces, a term appears (proportional to $(\omega/c)^2$) related to the medium compressibility.

The analysis of the equations and boundary conditions for the pulsating fields (3.37) shows that the non-homogeneities of the pulsation velocity, \mathbf{w} , are determined by three mechanisms. (i) Pulsation dispersion at the density inhomogeneities caused by non-isothermality. This mechanism takes place in the case of thermal vibrational convection in incompressible fluid and was analysed for the first time by Zenkovskaya & Simonenko (1966). Two other mechanisms are specific to the compressible medium. (ii) The first one is due to the effect of compressibility in the bulk (in the continuity equation) and was examined by Lyubimov (2000). (iii) The boundary condition for the pulsation velocity, besides the compressibility effect in the boundary layer, presupposes a critical divergence of the specific-heat ratio γ . This mechanism was first considered by Carles & Zappoli (1995).

Let us rewrite equations (3.36)–(3.37) and boundary conditions (3.38) in dimensionless form. The quantities L , L^2/χ , χ/L , θ , $a\omega$, $a\omega L$ are taken as the units of length, time, average velocity, temperature, pulsation velocity \mathbf{w}_0 and potential Φ . The pulsation field \mathbf{w} is represented as a sum of two components, with $\mathbf{w}^{(1)}$ related to the incompressible mechanism and $\mathbf{w}^{(2)}$ related to the medium compressibility. The measurement scale for \mathbf{w} is $2\nu\chi/(a\omega\beta\theta L^2)$. System (3.36)–(3.38) takes the form

$$\frac{1}{Pr} \left(\frac{\partial \mathbf{u}}{\partial t} + (\mathbf{u} \cdot \nabla) \mathbf{u} \right) = -\nabla \Pi + \Delta \mathbf{u} + RaT\gamma + ((\mathbf{w}^{(1)} + \mathbf{w}^{(2)}) \cdot \mathbf{w}_0) \nabla T + \frac{\sigma - 1}{2} Ra_a \Phi^2 \nabla T, \tag{3.42a}$$

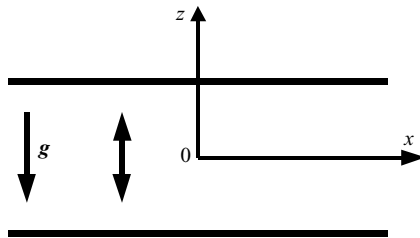


FIGURE 2. Plane layer.

$$\frac{\partial T}{\partial t} + (\mathbf{u} \cdot \nabla)T = \Delta T + \frac{\partial}{\partial t} \langle T \rangle, \quad \nabla \cdot \mathbf{u} = 0. \quad (3.42b)$$

The boundary conditions for the average fields are

$$T = T_B, \quad \mathbf{u} = 0. \quad (3.43)$$

The equations for the pulsation fields are

$$\nabla \times \mathbf{w}^{(1)} = Ra_v \nabla \times \mathbf{w}_0, \quad \nabla \cdot \mathbf{w}^{(1)} = 0; \quad (3.44a)$$

$$\nabla \times \mathbf{w}^{(2)} = 0, \quad \nabla \cdot \mathbf{w}^{(2)} = -Ra_a \Phi; \quad (3.44b)$$

$$\text{at the boundary: } w_n^{(1)} = 0, \quad w_n^{(2)} = Ra_{PE} \Phi. \quad (3.44c)$$

Equation (3.41) is rewritten in the form:

$$Ra_a \int_V \Phi \, dV + Ra_{PE} \oint_S \Phi \, dS = 0. \quad (3.45)$$

Equations (3.42)–(3.45) contain the following dimensionless parameters: the Prandtl number, the thermal Rayleigh number and three analogues of the Rayleigh number called ‘vibrational’, ‘acoustic’, and ‘near-critical’ Rayleigh numbers,

$$Pr = \frac{\nu}{\chi}, \quad Ra = \frac{g\beta\theta L^3}{\nu\chi}, \quad Ra_v = \frac{1}{2} \frac{(a\omega L)^2}{\nu\chi} (\beta\theta)^2, \quad (3.46)$$

$$Ra_a = \frac{1}{2} \frac{(a\omega L)^2}{\nu\chi} (\beta\theta) \left(\frac{\omega L}{c} \right)^2, \quad Ra_{PE} = \frac{1}{2} \frac{(a\omega L)^2}{\nu\chi} (\beta\theta) \left(\frac{\omega L}{c} \right)^2 \frac{\gamma\delta_\chi}{L}. \quad (3.47)$$

According to its definition, the usual thermal Rayleigh number is the relation between the work of the buoyancy force to displace a liquid element and the related dissipated energy. Similarly, the vibrational Rayleigh number characterizes the relation between the work done for the average displacement of a heated element by the pulsational flow and the energy which is dissipated; the acoustic Rayleigh number characterizes the work of the pressure force for compression of the fluid, and Ra_{PE} characterizes the adiabatic heating.

Based on the theoretical model obtained, we shall discuss several specific problems.

3.4. Plane horizontal layer

Let us consider the uniform vertical vibrations $\mathbf{w}_0 = \boldsymbol{\gamma} = -\mathbf{g}/g$ of a horizontal layer (figure 2). The thickness of the layer is taken as the length scale. We suppose that the walls are maintained at fixed temperatures: at the top $-1/2$, at the bottom $+1/2$ (the temperature difference θ between the walls is chosen as the temperature scale).

In the case under consideration the problem (3.42)–(3.45) allows a solution which corresponds to the state with zero average velocity, called the ‘quasi-equilibrium state’

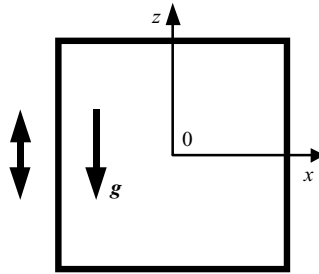


FIGURE 3. Square cavity.

(see Gershuni & Lyubimov 1998). In this state

$$T = -z, \quad \mathbf{w}^{(1)} = 0, \quad w_x^{(2)} = 0, \quad w_z^{(2)} = \frac{1}{2}Ra_a\left(\frac{1}{4} - z^2\right) - \frac{1}{2}Ra_{PE}. \quad (3.48)$$

Thus, two generation mechanisms can be distinguished for the pulsation field. The inhomogeneous component of the velocity $\mathbf{w}^{(2)}$ is caused by the compressibility in the bulk; the constant addition that leads to the bulk movement with respect to the walls is caused by compressibility in the boundary layer. The second mechanism results in a homogeneous fluid motion (like a solid body) when the bulk bounces back and forth between two highly compressible thermal boundary layers. Such motion of a near-critical fluid was first described by Carles & Zappoli (1995) (called the ‘quasi-solid regime’), who studied only the pulsating motion. In their work, the temperatures of both plates are equal, but this is not essential for such pulsating motion.

In (3.48) only the first term affects the stability of the quasi-equilibrium. The problem of stability was investigated by Lyubimov (2000) who showed that the effect of compressibility may generate convection even under microgravity conditions.

3.5. Square cavity

Let us examine the behaviour of a near-critical fluid in a square cavity subjected to uniform vertical vibrations: $\mathbf{w}_0 = \boldsymbol{\gamma} = -\mathbf{g}/g$, i.e. $\Phi = z$ (figure 3). We consider the two-dimensional problem, introducing the stream function ζ and vorticity Ω for the average velocity field:

$$u_x = \frac{\partial \zeta}{\partial z}, \quad u_z = -\frac{\partial \zeta}{\partial x}, \quad \Omega = \Delta \zeta. \quad (3.49)$$

The stream function ψ for pulsating field $\mathbf{w}^{(1)}$ and the potential ϕ for pulsating field $\mathbf{w}^{(2)}$ are also introduced as follows:

$$w_x^{(1)} = \frac{\partial \psi}{\partial z}, \quad w_z^{(1)} = -\frac{\partial \psi}{\partial x}, \quad \mathbf{w}^{(2)} = \nabla \phi. \quad (3.50)$$

Governing equations (3.42) rewritten in the new terms take the following form:

$$\frac{\partial \Omega}{\partial t} + \frac{1}{Pr} J(\Omega, \zeta) = \Delta \Omega - Ra^* \frac{\partial T}{\partial x} - Ra_v J\left(T, \frac{\partial \psi}{\partial x}\right) + Ra_{PE} J\left(T, \frac{\partial \phi}{\partial z}\right), \quad (3.51a)$$

$$Pr \frac{\partial}{\partial t}(T - \langle T \rangle) + J(T, \zeta) = \Delta T, \quad (3.51b)$$

$$\Delta \zeta = \Omega, \quad \Delta \psi = -\frac{\partial T}{\partial x}, \quad \Delta \phi = 0. \quad (3.51c)$$

Here

$$Ra^* = Ra - (\sigma - 2)zRa_a, \quad J(u, v) = \frac{\partial u}{\partial x} \frac{\partial v}{\partial z} - \frac{\partial u}{\partial z} \frac{\partial v}{\partial x}. \quad (3.52)$$

It is seen that, in equations (3.51), the influence of compressibility is reduced to an effective gravity force, dependent on the vertical coordinate: the temperature gradient and effective gravity force are in the same direction in half of a layer which makes the fluid stratification potentially unstable even under weightlessness. It is interesting that the dependence on the vertical coordinate is eliminated in the case of a perfect gas (when $\sigma = 2$), explained by the fact that the energy density of a standing wave is spatially homogeneous in a perfect gas. In the calculations presented below, $\sigma = 3$, which corresponds to the van der Waals equation of state.

The temperature is fixed at the horizontal walls and, at the vertical walls, the linear temperature distribution is maintained:

$$x = \pm \frac{1}{2}: \quad \zeta = 0, \quad \frac{\partial \zeta}{\partial x} = 0, \quad T = -z, \quad \psi = 0, \quad \frac{\partial \phi}{\partial x} = \pm z; \quad (3.53a)$$

$$z = \pm \frac{1}{2}: \quad \zeta = 0, \quad \frac{\partial \zeta}{\partial z} = 0, \quad T = \mp \frac{1}{2}, \quad \psi = 0, \quad \frac{\partial \phi}{\partial z} = \frac{1}{2}. \quad (3.53b)$$

Here, the boundary conditions follow from the general expressions (3.43) and (3.44).

First, we estimated the orders of the dimensionless parameters. A near-critical fluid at $\epsilon \sim 10^{-3}$ filling a square cavity with length $L \sim 1$ cm, subjected to vibrations with amplitude $a \sim 10^{-2}$ cm and frequency $\omega \sim 10^3$ s $^{-1}$ and to temperature difference $\theta \sim 10^{-3}$ K, is considered. For this case the non-dimensional parameters are of the following orders: $Ra \sim 10^9$, $Ra_v \sim 10^6$, $Ra_a \sim 10^5$, $Ra_{PE} \sim 10^4$, $Pr \sim 10^2$. Therefore, under terrestrial conditions, buoyancy convection predominates over all vibrational flows. Under microgravity conditions, vibrational convection might be stronger than that of buoyancy.

As one can see from (3.51)–(3.53), at non-zero values of Ra_{PE} the quasi-equilibrium state is impossible. The flow structures were examined numerically by the finite-difference method (implicit second-order scheme). The problem is characterized by too many parameters, and only some sections of parameter space were examined. The dependences of integral characteristics defining the flow intensity (the maximum value of stream-function, ψ_{max}) and the intensity of heat transfer (the Nusselt number, $Nu = - \int_{\Gamma} (\partial T / \partial n) dl$, where $\partial T / \partial n$ is a normal derivative of temperature at a boundary and integration is carried out over the whole cavity boundary) on parameters were obtained.

For an incompressible fluid in the absence of vibrations, this problem was considered by Gershuni, Zhukhovitsky & Tarunin (1966) and Gershuni & Zhukhovitsky (1976). The case of a compressible fluid with fixed Prandtl number ($Pr = 0.71$) in the absence of vibrations was examined by Polezhaev (1968).

First, we calculated the thermal convection assuming $Ra_a = Ra_{PE} = Ra_v = 0$ in equations (3.51) for a wide range of Prandtl numbers: $Pr = 1$ to ∞ (the limit $Pr \rightarrow \infty$ is of special interest for near-critical fluids, as it corresponds to $\epsilon \rightarrow 0$; this case was examined by neglecting the left-hand terms in the Navier–Stokes equation). It was found that, for Prandtl numbers ~ 1 , one-vortex flow is the main regime; at higher Prandtl numbers transitions between one-vortex and two-vortex patterns occur (figures 4 and 5). Hysteresis is observed for these transitions, as mentioned in the work of Lyubimova (1986), where the limit $Pr \rightarrow \infty$ was also examined.

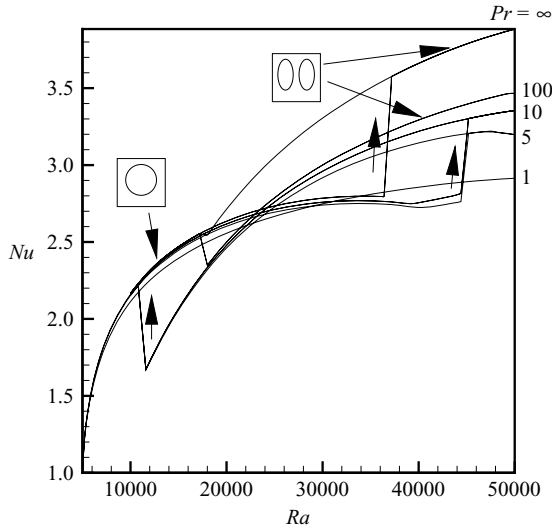


FIGURE 4. Heat flux vs. thermal Rayleigh number Ra (other Rayleigh numbers equal 0) at different Prandtl numbers.

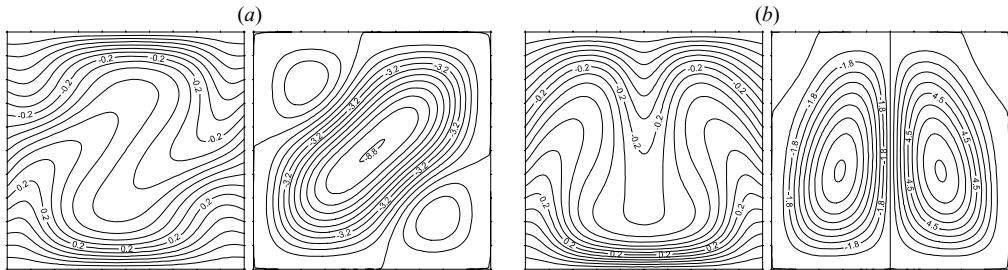


FIGURE 5. (a) One-vortex regime. Isotherms (left) and average flow pattern (right) at $Pr = 100$, $Ra = 4.5 \times 10^4$, other Rayleigh numbers equal zero. $Nu = 2.89$, $\psi_{max} = 8.83$. (b) Two-vortex regime. Isotherms and average flow pattern at $Pr = 100$, $Ra = 4.5 \times 10^4$, other Rayleigh numbers equal zero. $Nu = 3.52$, $\psi_{max} = 8.18$.

In figure 6 the intensities of pure ‘near-critical’ and pure ‘acoustic’ flows are plotted as functions of the corresponding Rayleigh numbers. Figure 7 presents the average flow structures and temperature fields. In both cases the flow has a two-vortex structure. The ‘near-critical’ mechanism always generates flow with ascending flux in the cavity centre. The ‘acoustic’ mechanism might induce flows in different directions; the intensities of these flows are slightly different. The coupling of the two mechanisms may lead either to reduction or to increase of the flow intensity in the lower part of the cavity. The flow in the upper part of the cavity is always damped out due to the ‘acoustic’ mechanism (see figure 8a)).

The calculations for coupled ‘acoustic’ or ‘near-critical’ mechanisms with buoyancy convection result in noticeable intensification of fluid motion and heat–mass transfer. Additionally, the ‘near-critical’ mechanism always generates flows with ascending flux, and imposes the preferred direction for the fluid motion. The coupling of ‘near-critical’ and buoyancy flow is shown in figure 8(b), and the interplay between ‘acoustic’ and buoyancy convective flows is given in figure 9.

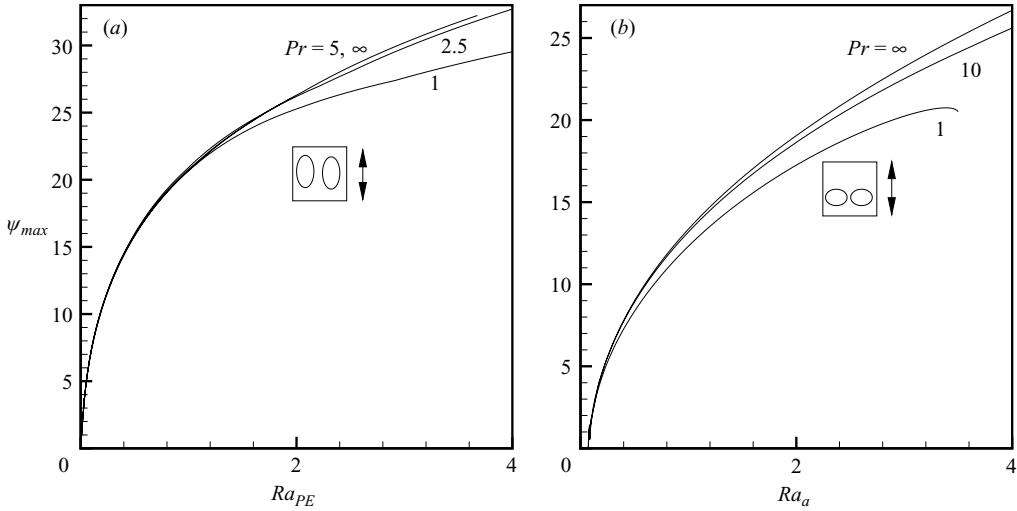


FIGURE 6. (a) Intensity of average flow vs. ‘near-critical’ Rayleigh number Ra_{PE} (other Rayleigh numbers equal 0) at different Prandtl numbers. (b) Intensity of average flow vs. ‘acoustic’ Rayleigh number Ra_a (other Rayleigh numbers equal 0) at different Prandtl numbers.

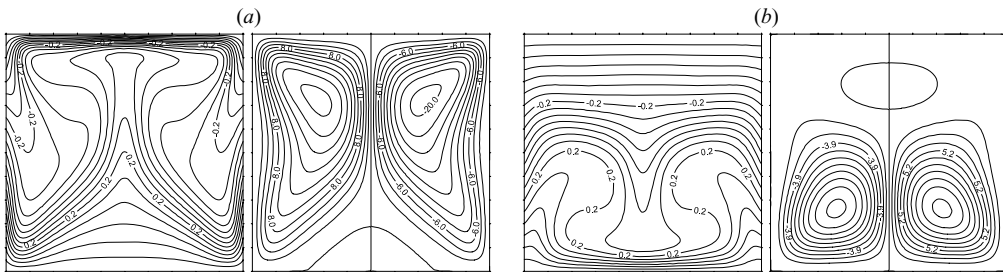


FIGURE 7. (a) Isotherms and average flow pattern at $Pr = 100$, $Ra_{PE} = 10^6$, other Rayleigh numbers equal zero. $Nu = 8.13$, $\psi_{max} = 20.6$. (b) Isotherms and average flow pattern at $Pr = 100$, $Ra_a = 2 \times 10^6$, other Rayleigh numbers equal zero. $Nu = 3.38$, $\psi_{max} = 13.3$.

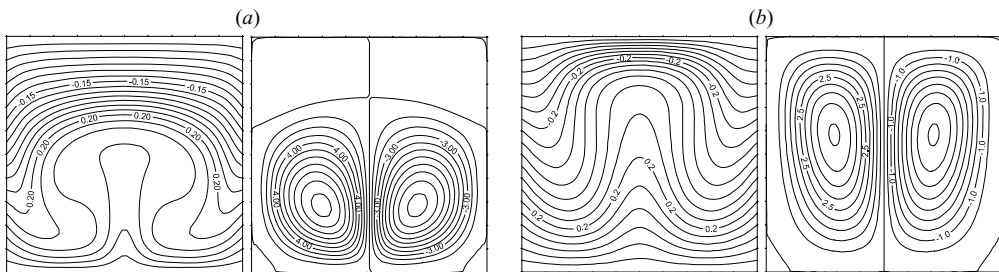


FIGURE 8. (a) Isotherms and average flow pattern at $Pr = 100$, $Ra_a = 10^6$, $Ra_{PE} = 10^5$, other Rayleigh numbers equal zero. $Nu = 2.53$, $\psi_{max} = 10.3$. (b) Isotherms and average flow pattern at $Pr = 100$, $Ra = 2 \times 10^4$, $Ra_{PE} = 10^3$, other Rayleigh numbers equal zero. $Nu = 2.64$, $\psi_{max} = 4.55$.

The vertical vibrations are known to stabilize equilibria which are potentially unstable under gravity. The simplest example is the stabilization of a pendulum in the equilibrium position when its centre of gravity is located above its suspension point. A similar effect in the theory of thermal vibrational convection has been demonstrated in

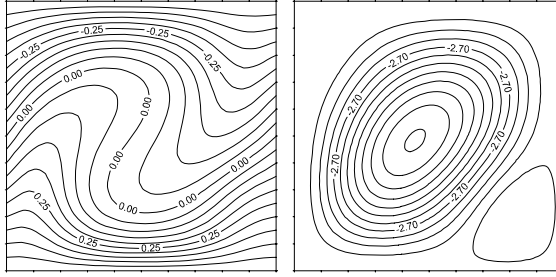


FIGURE 9. Isotherms and average flow pattern at $Pr = 100$, $Ra = 2 \times 10^4$, $Ra_a = 2 \times 10^4$, other Rayleigh numbers equal zero. $Nu = 2.56$, $\psi_{max} = 7.67$.

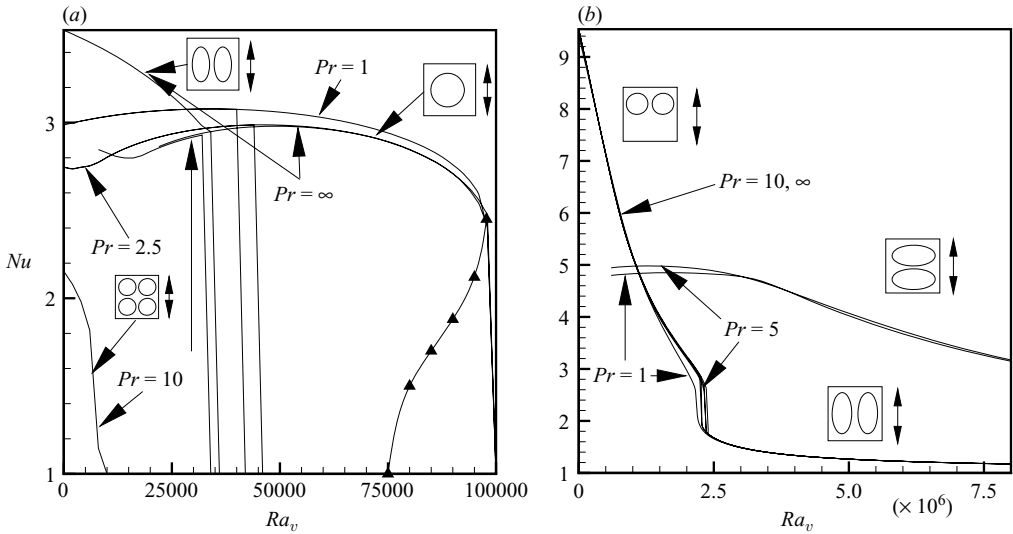


FIGURE 10. (a) Heat flux vs. vibrational Rayleigh number Ra_v ($Ra = 5 \times 10^4$, other Rayleigh numbers equal 0) at different Prandtl numbers. (b) Heat flux vs. vibrational Rayleigh number Ra_v ($Ra_{PE} = 10^6$, other Rayleigh numbers equal 0) at different Prandtl numbers. The curves were obtained both in ascending and descending directions of Ra_v . In the descending direction the curves usually lie on the ascending plots, but at $Pr = 1$ and $Pr = 5$ new structures, and correspondingly the new dependence, were found.

the first works on the linear stability of equilibria (Zenkovskaya & Simonenko 1966). Zaks, Lyubimov & Chernatynsky (1983) developed the weakly nonlinear analysis of the instability, and it was shown that stabilization occurs even with respect to finite disturbances. Moreover, if vibrations are strong enough, then the stabilization is absolute, i.e. the finite disturbances are damped at any Rayleigh number. This fact was confirmed in numerical simulations of thermal vibrational convection in a closed cavity carried out by Gelfgat (1991) (see also Gershuni & Lyubimov 1998, pp. 151–157). Figure 10 illustrates the analogous effect for thermal vibrational convection in near-critical fluid: when Ra_v increases, the intensity of convection decreases slowly, but when Ra_v reaches some threshold value, all disturbances are damped out and the asymptotic regime corresponds to an equilibrium state.

The interaction of the thermal vibrational mechanism with other types of convective flows also leads to a decrease of the motion intensity (figures 10 and 11).

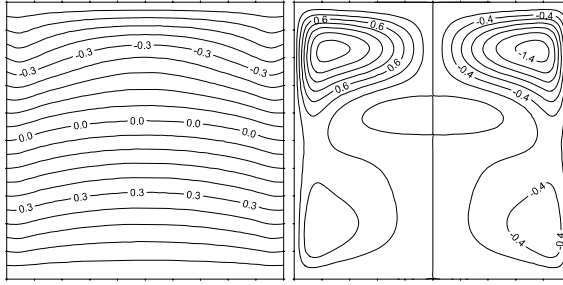


FIGURE 11. Isotherms and average flow pattern at $Pr = 100$, $Ra_{PE} = 10^6$, $Ra_v = 3 \times 10^6$, other Rayleigh numbers equal zero. $Nu = 1.30$, $\psi_{max} = 1.49$.

The problem was studied by the evolutionary method. It was found that different initial conditions (we carried out the computations with increasing a parameter and then decreasing) may result in steady flows of different patterns, which is also reflected in figures 10. Non-stable regimes obtained by a limitation technique (see Lyubimova 1974) are marked by triangles in figure 10(a).

We should emphasize the difference between the problem examined here and the works by Zappoli *et al.* (1996) and Polezhaev & Soboleva (2000), where the behaviour of near-critical fluid filling a square cavity was also studied. The main difference lies in the temperature boundary conditions. In the works mentioned, the temperature at the boundary is non-stationary. The authors are interested in transitional mechanisms taking place after heat impulse on a boundary. We, on the other hand, focus on the flows developing on long time scales (much longer than the typical scale of the piston effect) when all transitional processes have ended. The problem considered in this section is a classical problem of convective theory with typical boundary conditions (see Gershuni & Zhukhovitsky 1976), but with a non-classical fluid model.

3.6. Piston effect

Let us determine the equilibrium of a plane horizontal near-critical fluid layer in the absence of mechanical vibrations, under the following boundary conditions:

$$z = 0 : T = \cos \omega t; \quad z = 1 : T = 0. \quad (3.54)$$

The temperature distribution in a layer is determined by the equation:

$$\frac{\partial T}{\partial t} = \frac{\partial^2 T}{\partial z^2} + \frac{\partial}{\partial t} \langle T \rangle. \quad (3.55)$$

This means the temperature of a chosen fluid volume changes due to thermal conductivity and to the work of pressure forces of the surrounding fluid (for contractions or expansions the volume warms or cools). The second mechanism was first considered by Onuki *et al.* (1990).

Let us discuss two limiting cases.

(i) In the low-frequency case ($\omega \rightarrow 0$) the temperature distribution in a layer is trivial: $T = (1 - z) \cos \omega t$. This result may also be obtained without taking the term $\partial \langle T \rangle / \partial t$ into account.

(ii) In the case of high frequency of the external forcing ($\omega \rightarrow \infty$) if the term $\partial \langle T \rangle / \partial t$ is taken into account, the temperature distribution in a layer changes qualitatively. Without it, the temperature non-homogeneities remain bounded inside the boundary layer, whereas with it, the temperature in the bulk of a cavity is $T = \frac{1}{2} \cos \omega t$ (figure 12).

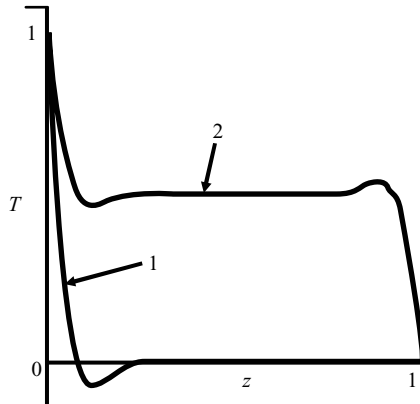


FIGURE 12. Temperature distribution in a plane layer subjected to strong non-stationary heating: (1) a normal fluid, (2) a near-critical fluid.

The case of synchronous temperature variations at the top and bottom walls is also interesting. Let us consider a more general formulation: let the temperature distribution be determined by

$$\frac{\partial T}{\partial t} = \frac{\partial^2 T}{\partial z^2} + \alpha \frac{\partial}{\partial t} \langle T \rangle. \quad (3.56)$$

Here $\alpha = 1$ corresponds to a near-critical fluid, and for a compressible fluid far from the critical point $\alpha \neq 1$. The following boundary conditions are imposed:

$$z = 0 : \quad T = \cos \omega t; \quad z = 1 : \quad T = \cos \omega t. \quad (3.57)$$

Then, the solution (in complex form) is as follows:

$$T = [A + B \cosh(k(z - 1/2))] \exp(i\omega t), \quad (3.58a)$$

$$B = \frac{(1 - \alpha)}{2\alpha \sinh(k/2)/k + (1 - \alpha) \cosh(k/2)}, \quad A = 1 - B \cosh(k/2), \quad (3.58b)$$

$$k = \sqrt{i\omega}, \quad \langle T \rangle = \frac{B}{\alpha} \exp(i\omega t). \quad (3.58c)$$

For the case of low frequencies ($k \rightarrow 0$), a layer is homogeneously heated; moreover, both $\langle T \rangle$ and $T \rightarrow \exp(i\omega t)$, and this result is independent of α .

For the case of high-frequency temperature variations ($k \rightarrow \infty$), a layer is not heated at all, $\langle T \rangle \rightarrow 0$, for any α , apart from $\alpha = 1$. When $\alpha \rightarrow 1$, $\langle T \rangle \rightarrow \exp(i\omega t)/(1 + \frac{1}{2}k(1 - \alpha))$, i.e. the result depends on which parameter, k or $(1 - \alpha)$, tends to its limiting value faster. When $\alpha = 1$ (for a near-critical medium) T is spatially uniform, $T = \exp(i\omega t)$, and therefore $\langle T \rangle = \exp(i\omega t)$.

The essence of the piston effect is clearly seen here. This effect is typical only for the cases of strong non-stationary local heating: the bulk temperature changes instantly causing changes of the wall temperature (instantly because fluid behaviour on the dissipative time scales is considered). The temperature distribution represented in figure 12 demonstrates that a convective instability for problems of this kind may appear only inside the boundary layer, which was noted by Polezhaev & Soboleva (2000).

4. Remarks

4.1. Imperfection of the wall heat conductivity

An imperfection of boundary conditions may substantially influence heat transfer in a near-critical fluid (see Jounet *et al.* 2000*b*). This frequently results in discrepancies between theoretical and experimental data and has to be taken into account in experimental set-ups.

The heat conductivity of near-critical fluids is small, which forces us to take into account the finiteness of the heat conductivity of shell walls. In this case, the temperature perturbations obey the following condition:

$$T_2 - a \frac{\partial T_2}{\partial z_{-1}} = 0, \quad a = \frac{\kappa}{\kappa_B} \frac{1-i}{\sqrt{2}} \sqrt{\frac{\chi_B}{\omega}} (\epsilon L)^{-1}, \quad (4.1)$$

where κ_B , χ_B are the heat conductivity and heat diffusivity of a wall. Heat inside the wall is assumed to spread diffusely; and the heat flux at the gas-wall boundary must be continuous.

The boundary condition modified in such a way leads to the following pulsating density distribution inside the boundary layer:

$$\tilde{\rho}_1 = -\frac{1}{1+b} \frac{\mu A}{p_{\rho T}} i \Phi \exp(-\beta z_{-1}), \quad b = \frac{\kappa}{\kappa_B} \sqrt{\frac{\chi_B}{\chi}}. \quad (4.2)$$

This brings us to the multiplication of some effective boundary conditions by a correction factor. Namely, condition (3.38) needs to be transformed to

$$w_n \rightarrow \frac{1}{1+b} w_n, \quad b = \frac{\kappa}{\kappa_B} \sqrt{\frac{\chi_B}{\chi}} \rightarrow \epsilon^{-(\Phi+\gamma)/2}. \quad (4.3)$$

The factor $(\Phi + \gamma)/2 = 0.9$ (where Φ is the singular factor, see §2), i.e. when approaching the critical point, the correction factor rapidly diverges.

4.2. Acoustic filtering

In accordance with Chenoweth & Paolucci (1986), Zappoli *et al.* (1996) and Polezhaev & Soboleva (2000), if the convective motion is slow, the average pressure field can be represented as a sum: $p = \bar{p}(t) + p'(t, \mathbf{r})$, where $\bar{p}(t)$, $p'(t, \mathbf{r})$ are the thermodynamic and dynamic pressure parts. The first term is determined by the whole fluid mass in the cavity and by the average temperature in the cavity. The second part is determined by the flow structure (usually ρu^2 , where ρ , u are typical values of density and average velocity). In the case of slow flows $\bar{p} \gg p'$.

The asymptotic equations presented in this work reflect all these facts. The term $\partial \langle T \rangle / \partial t$ in the energy equation only determines the thermodynamic component of the pressure field (the whole fluid mass is assumed constant). We also note that, in the case of a compressible fluid far from the critical point, this term must be multiplied by a factor $(\gamma - 1)/\gamma$, where γ is the specific-heat ratio (see Chenoweth & Paolucci 1986), which qualitatively changes some solutions: upon simultaneous heating of all the sides of an enclosure, in the case of $\alpha = 1$ the spatially uniform temperature distribution is the solution, whereas the thermal waves propagate near the walls for $\alpha \neq 1$ (see §3.6).

5. Conclusions

The main body of the present work is the development of a closed system of averaged equations for the convection in a non-uniformly heated near-critical fluid

subjected to translational vibrations. The model takes into account the anomalous behaviour of the thermodynamic and transport coefficients in the critical range. The main peculiarity of these equations is that boundary layers undergo strong thermoacoustic couplings which strongly modify the boundary conditions for the bulk fluid equations, which remain almost unchanged compared to those of normally compressible fluids. These boundary layer effects are shown to be responsible for most of the new behaviours which are found. These averaged equations have been validated through the good agreement of the results we obtained for previously studied problems such as thermoacoustic speeding up of the heat transport, gravitational convection and hydrodynamic instabilities.

We stress the fact that the equations obtained allow long-term exploration of the average components of convective flow properties under vibration and the stability which, until now, have been limited by the available computational time to short time scales and the oscillating component of the relevant fields at best.

In the present paper (Part 1), the imposed temperature difference is taken to be of the order $\theta = O(\epsilon^2)$. The heating here is an imposed external factor, which makes the density distribution non-homogeneous. A non-homogeneous density field is one of the necessary conditions for the appearance of average vibrational flows. However, even in isothermal conditions, owing to mechanical compressibility and pressure force work, mechanical vibrations or gravity stratification can cause small temperature differences, which are of the next smallness order compared to the external heating considered here. If, however, the imposed heating is assumed to be small, or even absent (isothermal boundary conditions), such temperature non-homogeneities may be important and result in additional mechanisms for the generation of vibrational flows. The next part of our work (see Part 2 Lyubimov *et al.* 2006) deals with slightly non-uniform heating, when $\theta = o(\epsilon^2)$, which includes the isothermal boundary conditions.

This work was supported by (i) Award No. PE-009-0 from the US Civilian Research & Development Foundation for the Independent States of the Former Soviet Union (CRDF); (ii) grant from the Russian Foundation for Basic Research No. 0001-00450; (iii) programme of financial support for Leading Scientific Schools, grants No. 00-15-96112 and NSh-1981.2003.1; (iv) within the framework of Reseau formation-recherche franco-russe of MENRT-DRIC.

REFERENCES

- BEYSENS, D. & GARRABOS, Y. 2001 Near-critical fluids under microgravity: status of the ESEME program and perspectives for the ISS. *Acta Astronautica* **48**, No. 5–12, 629–638.
- BOUKARI, H., SHAUMEYER, J. N., BRIGGS, M. E. & GAMMON, R. W. 1990 Critical speeding up in pure fluids. *Phys. Rev. A* **41**, 2260–2263.
- CARLES, P. & ZAPPOLI, B. 1995 The unexpected response of near-critical fluids to low-frequency vibrations. *Phys. Fluids* **7**, 2905–2914.
- CHENOWETH, D. R. & PAOLUCCI, S. 1986 Natural convection in an enclosed vertical air layer with large horizontal temperature differences. *J. Fluid Mech.* **169**, 173–210.
- GARRABOS, Y., BONNETI, M., BEYSENS, D., PERROT, F., FROHLICH, T., CARLES, P. & ZAPPOLI, B. 1998 Relaxation of supercritical fluid after a heat pulse in the absence of gravity effects: theory and experiments. *Phys. Rev. E* **57**, 5665–5682.
- GELFGAT, A. YU. 1991 Development and instability of steady convective flows in square cavity heated from below in the field of vertical vibrations. *Izv. Akad. Nauk. SSSR, Mekh. Zhid. i Gaza* N 2, 9–18 (in Russian).
- GERSHUNI, G. Z. & LYUBIMOV, D. V. 1998 *Thermal Vibrational Convection*. Wiley & Sons.

- GERSHUNI, G. Z. & ZHUKHOVITSKY, E. M. 1976 *Convective Stability of Incompressible Fluid*. Keter, Jerusalem.
- GERSHUNI, G. Z. & ZHUKHOVITSKY, E. M. 1981 On convective instability of fluid in vibrational field in weightlessness. *Izv. Akad. Nauk. USSR, Mekh. Zhid. i Gaza* **4**, 12–19 (in Russian).
- GERSHUNI, G. Z., ZHUKHOVITSKY, E. M. & TARUNIN, E. L. 1966 Numerical study of convection in a fluid heated from below. *Izv. Akad. Nauk. USSR, Mekh. Zhid. i Gaza* **6**, 93–99 (in Russian).
- GITTERMAN, M. SH. & STEINBERG, V. A. 1970 Criteria of occurrence of free convection in a compressible viscous heat-conducting fluid. *Problemy Mate. i Mekh.* **34**, issue 2, 325–331 (in Russian).
- JOUNET, A., MOJTABI, A., OUZZANI, J. & ZAPPOLI, B. 2000a Low-frequency vibrations in a near-critical fluid. *Phys. Fluids* **12**, 197–204.
- JOUNET, A., ZAPPOLI, B. & MOJTABI, A. 2000b Rapid thermal relaxation in near-critical fluids and critical speeding up: discrepancies caused by boundary effects. *Phys. Rev. Lett.* **84**, 3224–3227.
- LYUBIMOV, D. V. 1995 Convective flows under the influence of high-frequency vibrations. *Eur. J. Mech., B/Fluids* **14**, 439–458.
- LYUBIMOV, D. V. 2000 Thermal convection in an acoustic field. *Fluid Dyn.* **35**, 321–330.
- LYUBIMOV, D., LYUBIMOVA, T., VOROBEV, A., MOJTABI, A. & ZAPPOLI, B. 2006 Thermal vibrational convection in near critical fluids. Part 2. Weakly non-uniform heating *J. Fluid Mech.*, **564**, 185–196.
- LYUBIMOVA, T. P. 1974 Convection of non-Newtonian liquids in closed cavities heated from below. *Fluid Dyn. (Historical Archive)* **9**, 319–322.
- LYUBIMOVA, T. P. 1986 On steady solutions of convection equations for a visco-plastic fluid, heated from below, taking into account the temperature dependence of rheological parameters. *Vestsi Akad. Navuk BSSR, Serya fizika-energetychnyh navuk* **1**, Minsk, 91–96 (in Russian).
- ONUKI, A., HAO, H. & FERRELL, R. A. 1990 Fast adiabatic equilibration in a single-component fluid near the liquid-vapor critical point. *Phys. Rev. A* **41**, 2256–2259.
- POLEZHAEV, V. I. 1968 Flow and heat transfer with natural convection of a gas in a closed region after loss of hydrostatic equilibrium stability. *Izv. Akad. Nauk. SSSR, Mekh. Zhid. i Gaza* **3**, N 5, 124–129 (in Russian).
- POLEZHAEV, V. I., EMELIANOV, V. M. & GORBUNOV, A. A. 1998 Near-critical fluids in microgravity: concept of research and new results of convection modelling. *J. Japan Soc. Microgravity Appl.* **15**, Supplement II, 123–129.
- POLEZHAEV, V. I. & SOBOLEVA, E. B. 2000 Thermal gravitational and vibrational convection of near-critical gas under microgravity conditions. *Fluid Dyn.* **35**, N 3, 371–379.
- SCHLICHTING, G. 1968 *Boundary Layer Theory*. McGraw-Hill.
- SPIEGEL, E. A. 1965 Convective instability in a compressible atmosphere I. *Astrophys. J.* **141**, 1068–1090.
- STANLEY, H. E. 1971 *Introduction to Phase Transitions and Critical Phenomena*. Clarendon.
- ZAKS, M. A., LYUBIMOV, D. V. & CHERNATYNSKY, V. I. 1968 On the influence of vibrations on the regimes of supercritical convection. *Izv. Akad. Nauk. SSSR, Fizi. Atmosf. i Okean.* N 3, 312–314 (in Russian).
- ZAPPOLI, B., AMIROUDINE, S., CARLES, P. & OUZZANI, J. 1996 Thermoacoustic and buoyancy-driven transport in a square side-heated cavity filled with a near-critical fluid. *J. Fluid Mech.* **316**, 53–72.
- ZAPPOLI, B., BAILLY, D., GARRABOS, Y., LE NEINDRE, B., GUENOUN, P. & BEYSENS, D. 1990 Anomalous heat transport by the piston effect in supercritical fluids under zero gravity. *Phys. Rev. A* **41**, 2264–2267.
- ZAPPOLI, B. & CARLES, P. 1996 Acoustic saturation of the critical speeding up. *Physica D* **89**, 381–394.
- ZENKOVSKAYA, S. M. & SIMONENKO, I. B. 1966 On the effect of high-frequency vibrations on the origin of convection. *Izv. Akad. Nauk. SSSR, Mekh. Zhid. i Gaza* **5**, 51–55 (in Russian).